

Nanosatellite Attitude Control System for the Oculus: A Space-Based Imaging Platform for Space Situational Awareness

Mary Farmer, Gordon Parker, Lyon B. King, Peter Radecki, Jeff Katalenich
 Mechanical Engineering – Engineering Mechanics, Michigan Technological University
 1400 Townsend Dr., Houghton, MI; (906) 487-2551

mcfarmer@mtu.edu, ggparker@mtu.edu, lbking@mtu.edu, pradecki@mtu.edu, jakatale@mtu.edu

ABSTRACT

Space situational awareness (SSA) with in-space imaging is one of the top priorities of the U.S. military. The Oculus is a low-cost test bed for nanosatellite in-space imaging technologies. The purpose of the Oculus is to (1) demonstrate vision-based attitude control for tracking resident space objects (RSOs), (2) provide in-space validation of two imaging devices, and (3) train future space-systems engineers through both undergraduate and graduate student research and development. One of the major challenges of creating a low-cost nanosat imaging test bed is the three-axis attitude control system. The Oculus' mission requires two types of attitude control: inertially referenced attitude control and visually referenced attitude control. The visually referenced attitude control, focused upon in this paper, requires precise RSO tracking where both a wide field-of-view imager and a narrow field-of-view imager are used to provide feedback for visual servoing of the spacecraft. Such precise attitude control is implemented using reaction wheels. This paper describes the control strategies used for Oculus' attitude control for visual servoing. Closed-loop performance is illustrated using a dynamic simulation of the spacecraft and a hardware-in-the-loop test bed utilizing a Stewart platform.

INTRODUCTION

As a part of the University Nanosatellite Program, students at Michigan Technological University have been developing and building a nanosatellite (nanosat) for Space Situational Awareness. The University Nanosatellite Program (UNP) is sponsored by the Air Force Research Lab (AFRL) and the American Institute of Aeronautics and Astronautics (AIAA), and is funded by the Air Force Office of Scientific Research. The UNP Nanosat-5 Competition allows undergraduate and graduate students at 11 universities across the United States to take part in a satellite competition with the purpose of training next-generation engineers for the space industry. Each institution's satellite mission is unique and created to advance small satellite research and development in an area of interest to the AFRL. Michigan Tech's satellite, the Oculus, is outfitted with two visible imagers and a precise three-axis attitude control system for the purpose of Space Situational Awareness.

SPACE SITUATIONAL AWARENESS

For the U.S. space force, "Space Situational Awareness means knowing the location of every object orbiting the earth, active or inactive, big or small; and knowing why it is there, what it is doing now, and what we think it will be doing in the future."¹ SSA has become a matter of increasing importance as access to space has become easier. The U.S. has significant military and commercial assets in space that must be protected.

There are two main ways for the U.S. to reduce risk for space assets through SSA:¹

- 1) Identify and monitor hazards
- 2) Increase the robustness of the U.S. space force.

The United States' primary means of identifying and monitoring hazards in space is ground-based. The current technology, radio detection and ranging, (RADAR), is well suited for objects in low Earth orbit (LEO), with altitudes less than 2,000km. Space objects in higher orbits are more easily detected with optical telescopes, as they are normally solar illuminated.¹ Defense Advanced Research Projects Agency (DARPA) is currently working on new optical telescopes with wide fields-of-view to scan and search for objects beyond LEO. According to Lt. Col. Showmaker, however:

No matter how good a ground based telescope you build, there will always be times when your telescope is in daylight or under clouds, giving you gaps in your coverage. We're looking at a space-based system to augment ground-based SSA. This space based system would fill in the gaps when the ground-based telescope is unavailable, and more importantly, enable continuous tracking of suspicious objects.¹

The Oculus Role in SSA

The Oculus nanosat is designed to detect and monitor solar illuminated objects for space-based SSA. Students teamed with Raytheon Missile Systems and Science Applications International Corporation (SAIC) to incorporate an onboard imaging system with both narrow field-of-view (NFOV) and wide field-of-view (WFOV) capability. The onboard NFOV imager is extremely sensitive in low-light conditions and thus can be used to monitor space objects for the entire orbit per the requirements of SSA. The primary goal of the Oculus mission is a technology demonstration of this imager by acquiring, imaging, tracking, and monitoring space objects. To ensure that the Oculus has this opportunity, the nanosat design incorporates two deployable targets referred to as "cubesats." Additionally, the team will request an orbit similar to that of the International Space Station (ISS). A conjunction analysis, performed by students working on the project, using Satellite Tool Kit, determined that an orbit similar to that of the ISS would provide a multitude of imaging access windows of existing space objects, providing additional opportunities to further demonstrate the NFOV imager.

The Oculus' imaging mission is directly dependent on a precise three-axis attitude controlled platform. Such complex attitude control systems are uncommon on nanosats due to size and power restrictions. The development of proven, precision three-axis control on nanosat platforms could allow for many tasks normally restricted to microsatellites to be allocated to nanosats. Nanosats are becoming increasingly common in space applications because they are more economical to build and launch. The technology displayed by the Oculus also applies to the concept of increasing the robustness of the U.S. space force. One method of achieving this national goal is to reduce the potential impact of a disabled satellite by allocating individual tasks to a number of nanosats as opposed to having one larger satellite with several purposes. A fleet of nanosats with low-light-sensitive imagers and precise three-axis control have the potential to fulfill U.S. SSA requirements by supplementing the ground-based observation system and by distributing the task across many satellites.

STUDENT INVOLVMENT/ORGANIZATION

The UNP competition is unique in the opportunity that it provides to undergraduate engineers: very few undergraduates have the chance to contribute to the development of a satellite with a legitimate opportunity for launch into space. When the UNP competition concludes in January 2009, the AFRL seeks a launch opportunity for the winning entry. At Michigan Tech, the program's goal of training engineers for the future

workforce is being accomplished through the university's Enterprise Program.² During the 2008 spring semester, more than 80 undergraduate students, organized into eight separate teams, worked on the Oculus project. The project is multidisciplinary involving students majoring in electrical and mechanical engineering, business administration, software engineering, and materials science.

The project organization for the Oculus is unique. While most engineering universities have a senior capstone design project, Michigan Tech offers the Enterprise program that encourages students to get involved in a project as early as their sophomore year. The Oculus project is a part of the Aerospace Enterprise, meaning that all Oculus members are working on the project for credits that apply toward their degree. This has allowed the team to have a large, dedicated member base.

SATELLITE SYSTEM CONFIGURATION

In this section the Oculus' attitude control components are described in relationship to the satellite's modes of operation. First, an overview of the Oculus mission is given, emphasizing its mode-dependent attitude control objectives. This is followed by a description of the specific sensors and actuators selected. Finally, a description of how the attitude control components are used to satisfy the attitude control objectives is given.

The Oculus will be separated from its launch vehicle with an expected 6 degrees/second rotation in all three body axes. The first objective of the attitude control system is to detumble the spacecraft. After stabilizing the craft and establishing ground station communication, the Oculus will attempt to track self-deployed cubesats. The final objective is to test its tracking capability on a known target such as the ISS.

Sensors

The Oculus sensor suite consists of a three-axis gyroscope, a three-axis magnetometer, and a vision system. The gyroscope and magnetometer, shown in Figure 1, are used for inertially referenced attitude estimation and closed loop attitude control, exclusive of target tracking. The vision system consists of two cameras. The WFOV camera is used to identify the general location of a target. The NFOV, lowlight camera is used in conjunction with closed loop visual servoing to track the identified targets.

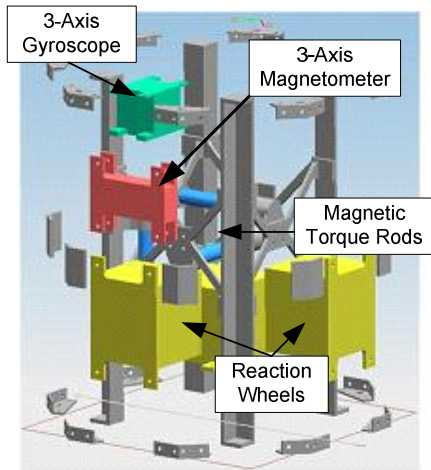


Figure 1 - Oculus Sensing and Actuation Hardware

Actuators

The spacecraft has both a magnetic torque rod system and a reaction wheel system for applying control moments to the satellite. The magnetic torque rods are used for both detumble and non-tracking attitude control along with desaturating the reaction wheels. The reaction wheels, shown in Figure 1, are used for attitude control during visual tracking operations due to their higher level of precision control.

Mission Evolution

The Oculus attitude control hardware was selected based on its ability to accomplish and fit within the mission goals, budget, and framework. A diagram of

the attitude control system is shown in Figure 2.

Initial detumbling of the satellite will occur with the magnetic torque rods. The control system will read in magnetometer data and use this to control the torque rods to drive the gyroscope rotational velocity to zero.

The Oculus satellite will have an onboard orbital model of its current position and magnetic field model of the earth. A Kalman filter attitude estimator will couple these two models along with the magnetometer and gyroscope reading to inertially reference its attitude.

The first mission objective will be to orient the satellite's antennas for ground communication. This maneuver will be conducted multiple times throughout mission lifetime for uploading commands to the satellite and downloading of stored images.

The SSA objectives will all follow a similar control path. First, the satellite will use the reaction wheels to point its imagers at an expected target and start capturing images. The images will be analyzed autonomously by onboard image recognition and tracking software. Once an object is identified, the 3-axis control system will transition from being inertially referenced to being visually referenced. This handoff will change what is producing the attitude control error but will not change the control laws which govern the reaction wheels. Throughout the visual tracking operation the control system will continually save images to disk while keeping the object centered in the camera's field of view.

External disturbance torques, which are predicted to be small because of the spacecraft's geometry, will be detected as a standard attitude error by the control

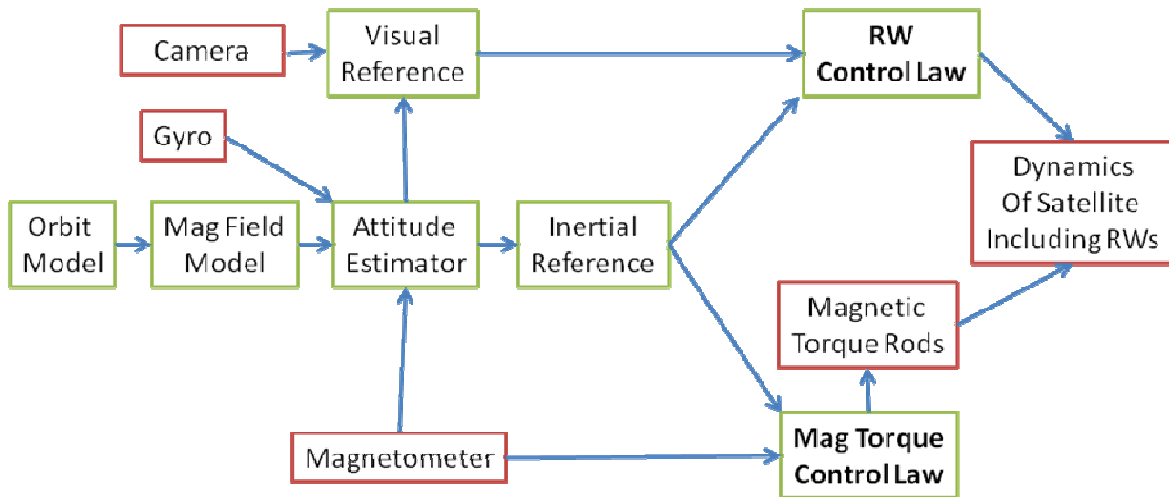


Figure 2 - Attitude Determination and Control Overview

system and automatically mitigated.³ The magnetic torque rods will desaturate reaction wheels during non-manuevering operational times when reaction wheels have unnecessary momentum.

The following section focuses on the reaction wheel control of the satellite used during visual servoing.

DYNAMICS AND KINEMATICS

The first step in designing and simulating the reaction wheel control system necessary for visual servoing is developing the equations of motion for the dynamics of the satellite. The dynamics incorporate both the satellite structure and the reaction wheels. The Oculus has three identical reaction wheels all mounted orthogonally to each other. The reaction wheel configuration is shown in Figure 3. The body coordinate frame is selected so each body axis is aligned with a spin axis of a reaction wheel.

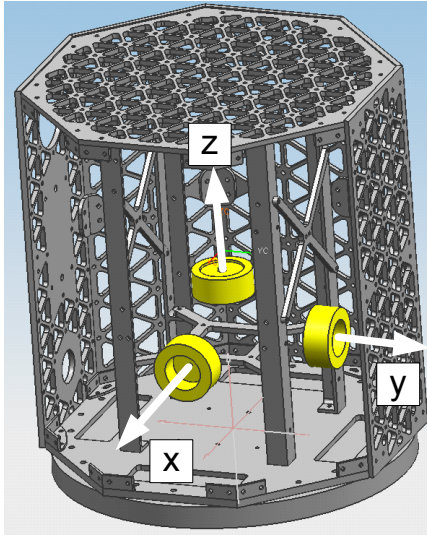


Figure 3 - Oculus Reaction Wheel Configuration

The moment of inertias about the spin axis of all three reaction wheels are combined into one inertia matrix, J , shown in Eq. (1)

$$J = \begin{bmatrix} J_{s1} & 0 & 0 \\ 0 & J_{s2} & 0 \\ 0 & 0 & J_{s3} \end{bmatrix} \quad (1)$$

where J_{s1} , J_{s2} , and J_{s3} , are the spin axis inertias of the reactions wheels aligned with the body frame x-axis, y-axis, and z-axis respectively.

The inertia matrix of the satellite without the inertias of the spin axes of the reaction wheels is defined as I and is shown in Eq. (2)

$$I = \begin{bmatrix} I_{11} & I_{12} & I_{13} \\ I_{12} & I_{22} & I_{23} \\ I_{13} & I_{23} & I_{33} \end{bmatrix} \quad (2)$$

The analysis of the satellite dynamics begins with the total angular momentum, H , show in Eq. (3)

$$H = I\omega + J(\omega + \Omega) \quad (3)$$

$$= (I + J)\omega + J\Omega$$

where ω is the absolute angular velocity of the satellite and Ω is the sum of the angular velocities of the reaction wheels relative to the satellite body frame about their spin axes and is given in Eq. (4)

$$\Omega = \Omega_1 b_1 + \Omega_2 b_2 + \Omega_3 b_3 \quad (4)$$

Next, the angular momentum of Eq. (3), is differentiated with respect to time to yield the attitude dynamic equations shown in Eq. (5)

$$M = \dot{H} + \omega \times H \quad (5)$$

$$= (I + J)\dot{\omega} + J\dot{\Omega} + \omega \times ((I + J)\omega + J\Omega)$$

where M is a vector of external moments. The relationship between the reaction wheel motor torques, T , and the angular acceleration is given in Eq. (6)

$$T = J(\dot{\omega} + \dot{\Omega}) \quad (6)$$

Attitude Kinematics

The attitude of the satellite can be represented using Euler parameters. Euler parameters describe attitude by defining a unit vector, r , and a rotation about that vector, Φ as defined in Eq. (7)

$$e_1 = r_1 \sin \frac{\Phi}{2} \quad e_2 = r_2 \sin \frac{\Phi}{2} \quad (7)$$

$$e_3 = r_3 \sin \frac{\Phi}{2} \quad e_4 = \cos \frac{\Phi}{2}$$

where the four Euler parameters are not independent and are related through Eq. (8)

$$e_1^2 + e_2^2 + e_3^2 + e_4^2 = 1. \quad (8)$$

The Euler parameter representation of attitude related to the angular velocity of the satellite is given in Eq. (9)

$$\begin{bmatrix} \omega_1 \\ \omega_2 \\ \omega_3 \\ 0 \end{bmatrix} = 2\tilde{e} \begin{bmatrix} \dot{e}_1 \\ \dot{e}_2 \\ \dot{e}_3 \\ \dot{e}_4 \end{bmatrix} \quad (9)$$

where

$$\tilde{e} = \begin{bmatrix} e_4 & e_3 & -e_2 & -e_1 \\ -e_3 & e_4 & e_1 & -e_2 \\ e_2 & -e_1 & e_4 & -e_3 \\ e_1 & e_2 & e_3 & e_4 \end{bmatrix} \quad (10)$$

To ensure that the Euler parameter constraint in Eq. (8) is satisfied during simulation, Baumgarte stabilization is used.⁵ Equation (9) is modified as shown in Eq. (11) where c is the pole location of the stabilization dynamics.

$$\begin{bmatrix} \omega_1 \\ \omega_2 \\ \omega_3 \\ c(e_1^2 + e_2^2 + e_3^2 + e_4^2 - 1) \end{bmatrix} = 2\tilde{e} \begin{bmatrix} \dot{e}_1 \\ \dot{e}_2 \\ \dot{e}_3 \\ \dot{e}_4 \end{bmatrix} \quad (11)$$

While an Euler parameter description is used for simulation, a modified Rodrigues parameter (MRP) representation of the attitude is used in the control laws. MRPs are more elegant for use in a controller because they are a three parameter representation of attitude. They relate to Euler parameters as shown in Eq. (12), (13) and (14).

$$\sigma_1 = \frac{e_1}{1+e_4} \quad \sigma_2 = \frac{e_2}{1+e_4} \quad \sigma_3 = \frac{e_3}{1+e_4} \quad (12)$$

$$\begin{aligned} e_1 &= \frac{2\sigma_1}{1+\sigma^T\sigma} & e_2 &= \frac{2\sigma_2}{1+\sigma^T\sigma} \\ e_3 &= \frac{2\sigma_3}{1+\sigma^T\sigma} & e_4 &= \frac{1-\sigma^T\sigma}{1+\sigma^T\sigma} \end{aligned} \quad (13)$$

MRPs have a singularity that exists at a rotation of 360 degrees where e_4 is equal to -1. To deal with this singularity Schaub and Junkins introduce shadowed

MRPs which represent a rotation in the opposite direction to the same orientation, as given in Eq. (14)⁶

$$\sigma_1^s = \frac{-e_1}{1-e_4} \quad \sigma_2^s = \frac{-e_2}{1-e_4} \quad \sigma_3^s = \frac{-e_3}{1-e_4} \quad (14)$$

The shadowed MRPs are used when $|\sigma|$ is greater than one.

REACTION WHEEL CONTROL

The reaction wheel controller, based on Lyapunov's direct method, was developed by Schaub and Junkins.⁶ For completeness, it is presented below.

The controller development starts with the following positive definite, radially unbounded, Lyapunov function shown in Eq. (15).

$$V(\sigma, \delta\omega) = \frac{1}{2} \delta\omega^T I \delta\omega + 2K \ln(1 - \sigma^T \sigma) \quad (15)$$

where $\delta\omega$ is the error in absolute angular velocity, σ is the MRP representation of the rotation from the desired attitude to the actual attitude and K is the positive definite gain matrix. The derivative of Eq. (15) is given in Eq. (16)

$$\dot{V}(\sigma, \delta\omega) = \delta\omega^T I \frac{d^B}{dt} \delta\omega + \delta\omega^T K \sigma \quad (16)$$

According to Lyapunov's direct method, to ensure stability, the derivative of Eq. (15) must be negative. Thus, Eq. (16) is set equal to a negative definite function as shown in Eq. (17)

$$\dot{V}(\sigma, \delta\omega) = -\delta\omega^T P \delta\omega \quad (17)$$

where P is a positive definite angular velocity gain matrix. Substituting $\dot{\omega} - \dot{\omega}_r + \omega \times \omega_r$ for $\frac{d^B}{dt} \delta\omega$ gives:

$$I \dot{\omega} = -K \sigma - P \delta\omega + I(\dot{\omega}_r - \omega \times \omega_r) \quad (18)$$

Substituting Eq. (5) and (6) into Eq. (18) gives Eq. (19)

$$\begin{aligned} & -\omega \times I \omega - \omega \times J(\omega + \Omega) - T + M \\ & = -K \sigma - P \delta\omega + I(\dot{\omega}_r - \omega \times \omega_r) \end{aligned} \quad (19)$$

The motor torque, T , can now be solved for:

$$T = -\omega \times I \omega - \omega \times J(\omega + \Omega) + M + K\sigma + P\delta\omega - I(\dot{\omega}_r - \omega \times \omega_r) \quad (20)$$

REACTION WHEEL CONTROL SIMULATION

Three different reaction wheel simulations are presented in this section. The first is an inertial attitude change, the second is inertial attitude tracking, and the final is a simulated object flyby.

The Oculus dynamics of Eq. (5) and (6) and the controller of Eq. (20) were simulated using Simulink and modeled with custom C-coded S-functions. This method of modeling allows for more direct porting of control laws to C-language satellite flight code.

For all the simulations, the mass properties of Table 1 were used.

Table 1: Reaction Wheel Mass Properties (kg m²)

I ₁₁	1.61725	I ₁₂	-0.01700
I ₂₂	1.31325	I ₁₃	-0.07600
I ₃₃	1.09700	I ₂₃	-0.00100

The spin axis inertia for each reaction wheel is 0.00188 kg m².

The reaction wheel controller gains were set to $K=40E$ and $P=10E$ to simply demonstrate the controller performance, where E is the identity matrix. In the future, actual controller gains will be set based on the controller's ability to meet mission performance objectives.

Inertial Attitude Change

The first simulation, analogous to a step response, is an inertial attitude change where the satellite is initially pointing in one direction and changes to point in another.

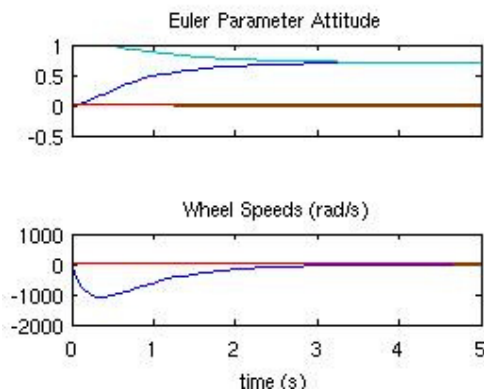


Figure 4 – Single-Axis Rotation

The satellite is initially at rest and pointing so that the body frame is aligned with the fixed frame. In this position the Euler parameter attitude is [0 0 0 1]. The satellite is then rotated 90 degrees about the body x-axis to the new Euler parameter attitude of [.707 0 0 .707]. The satellite has a first order-like response with no overshoot as shown in Figure 4.

Next, a three-axis maneuver is considered. The satellite was initially at rest and aligned with the fixed frame. The satellite completes a 3-1-3 rotation of 84.4 degrees, 66.4 degrees and -166.2 degrees to the Euler parameter attitude of [-.3162 .4472 -.5477 .6325]. Again, there is a first order-like response as shown in Figure 5.

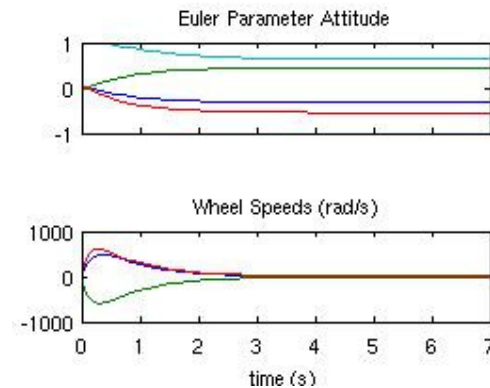


Figure 5 - Three-Axis Rotation

Inertial Attitude Tracking

The ability of the satellite to track a constant rate and change inertial attitude is simulated next. In these simulations the satellite starts at rest. In this first tracking simulation the satellite is commanded to spin at .3 rad/s around the body x-axis.

Within a few seconds the satellite catches up with the desired spin rate and has a pointing error of approximately zero as shown in Figure 6. From this it can be inferred that the system type is two or greater. In another simulation, not included in this paper, a constant acceleration was tracked with a steady state offset in attitude. This confirms the system is type two.

Next, rate tracking about all three-axes is considered. The satellite was commanded to spin at .1 rad/s about the body x-axis, -.2 rad/s about the body y-axis and .2 rad/s about the body z-axis. The results of this are shown in Figure 7 and match the results of the single-axis rate tracking.

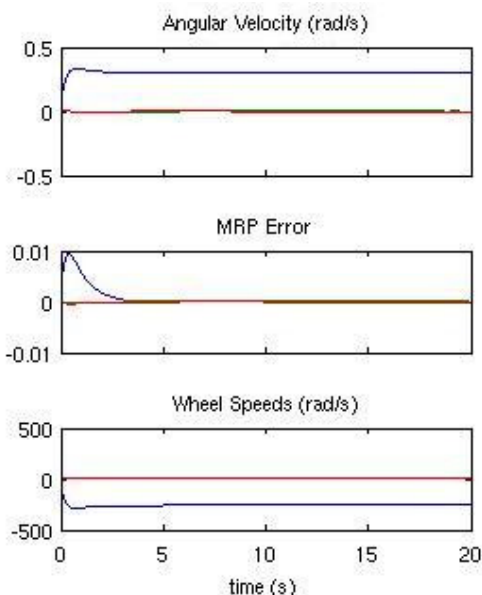


Figure 6 - Single-Axis Rate Tracking

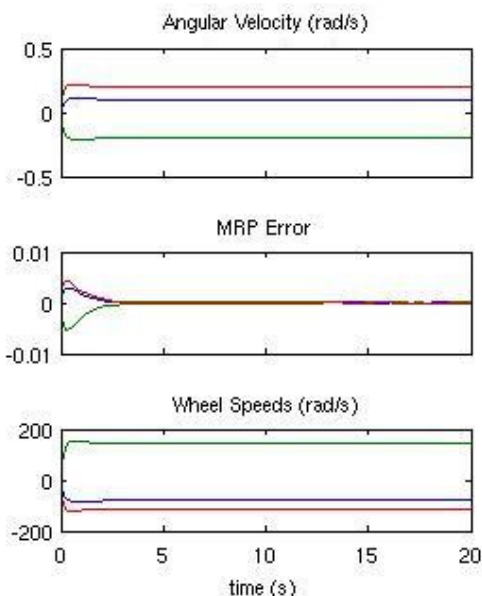


Figure 7 - Three Axis Rate Tracking

Simulated Flyby

The final simulation case is a flyby. The flyby illustrates the attitude rates necessary to track an object that starts at a position of [0 10 1] and moves in a straight line and at a constant velocity to a position of [0 -10 1] in two minutes. This is the same as having an object 1 km from the satellite moving by the satellite at 600 km/h.

Because the system is type two, the satellite is able to track systems with zero acceleration without steady state error. Tracking non-zero accelerations results in pointing errors in the attitude with the greatest error occurring where there is the greatest acceleration.

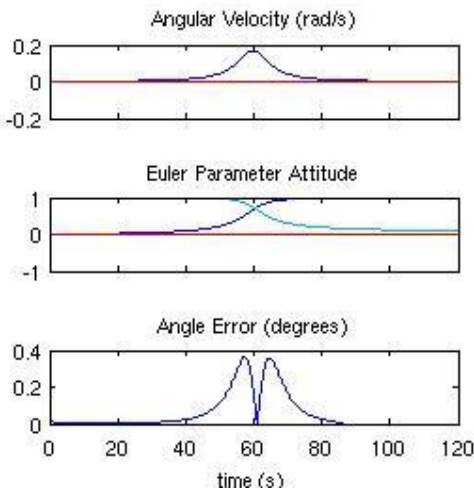


Figure 8 - Simulate Flyby Tracking

Figure 8 shows the results from the flyby simulation. As expected, the attitude error was greatest when the magnitude of the slope of the absolute angular velocity was the greatest, at approximately 56 and 62 seconds.

The maximum error in this test case is less than 0.4 degrees. It should be noted that the expected field of view on the Oculus NFOV imager is 8 degrees thus the 0.4 degree error is sufficient to keep imaging target within the field of view.

IMAGING TESTBED AND PERFORMANCE

Simulation, shown in the previous section, is one way of demonstrating and testing the Oculus attitude control system. To further prove and demonstrate the control system, simulations integrated with a hardware-in-the-loop test bed were conducted.

The Stewart platform, a six-degree-of-freedom rotation/translation table, was chosen as the test bed for the Oculus. Only the rotational capabilities of the platform were used for simulating the Oculus' attitude control system.

Stewart Platform Description

The Stewart platform is a parallel manipulator that consists of an upper and lower surface connected by six legs as shown in Figure 9. The orientation of the upper platform relative to the lower platform is achieved by changing the lengths of the legs of the platform. The

forward and inverse kinematics of the Stewart platform are presented by Huang.⁷

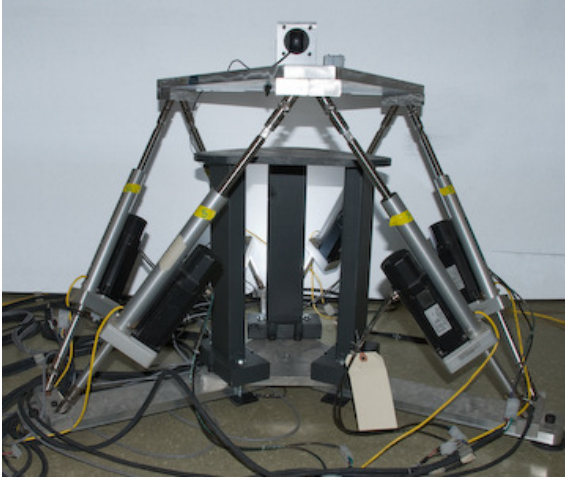


Figure 9 - Stewart Platform Setup

The first step in calculating the leg lengths using the Euler parameter attitude is to assign coordinate frames to the base, {B}, and the top, {T}, of the platform. Using these coordinate frames, vectors from the origin to each attachment point are found.

Next, the attachment point vectors of the top plate in the {T} frame are rotated using the rotation matrix in Eq. (21)

$$R = \begin{bmatrix} e_4^2 + e_1^2 - e_2^2 - e_3^2 & 2(e_1e_2 + e_4e_3) & 2(e_1e_2 + e_4e_3) \\ 2(e_1e_2 + e_4e_3) & e_4^2 - e_1^2 + e_2^2 - e_3^2 & 2(e_1e_2 + e_4e_3) \\ 2(e_1e_2 + e_4e_3) & 2(e_1e_2 + e_4e_3) & e_4^2 - e_1^2 - e_2^2 + e_3^2 \end{bmatrix}. \quad (21)$$

The vector from the base platform to the top platform when the platform is at its zero position is added to the rotated top platform attachment point vectors. If a

translation in addition to a rotation was desired it would also be added at this point. The results of these calculations are vectors to the top plate attachment points represented in the base frame.

To get the leg length measurements, the vector to the base attachment point is subtracted from the respective top attachment point and the magnitude of the resulting vector is found. The Stewart platform uses a proportional-derivative (PD) controller to control the leg lengths.

Model-Hardware Integration

The Stewart platform utilized the satellite and reaction wheel dynamics simulation to command its orientation. Figure 10 shows the hardware in-the-loop setup used with the Stewart platform.

The control strategy used for the visual servoing was a regulator which drives the pixel error from the images to zero. This pixel error, p , is converted to an angle error using Eq. (22)

$$\theta = \tan^{-1}\left(\frac{p}{808}\right). \quad (22)$$

The value, 808, is the virtual length of the adjacent leg of a right triangle in pixels, while the pixel error, p , is the length of the opposite leg. This angle error, converted to a MRP, is the input to the reaction wheel controller.

The reaction wheel controller calculates the reaction wheel torques required to drive the pixel error to zero. The satellite and reaction wheel dynamics and kinematics simulates the rotation of the satellite based on these torques. The result of the simulated satellite and reaction wheels is an Euler parameter representation of the satellite attitude. The Stewart platform uses the Euler parameter representation of attitude to orientate the vision system attached to it.

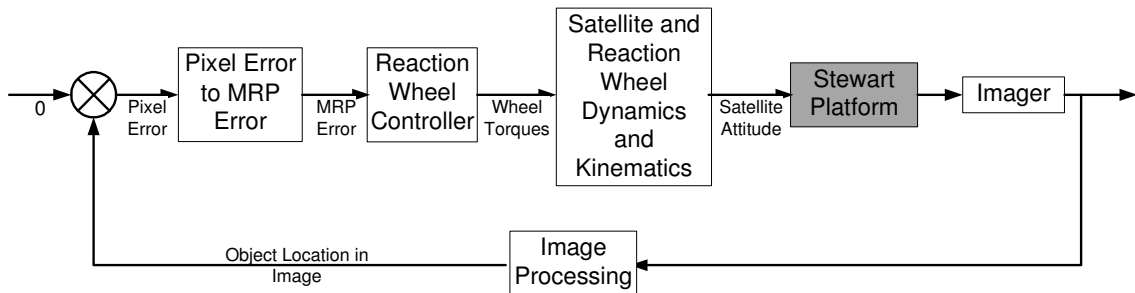


Figure 10 - Stewart Platform Hardware-in-the-loop Diagram

The vision system acquires images that are used to generate the target location in pixels. The vision system is aligned so that a vertical pixel error represents a rotation about the body y-axis and a horizontal pixel error represents a rotation about the body z-axis.

Stewart Platform Performance

The Stewart platform performance is demonstrated using a stationary imaging target. Future work will include setting up a projection system to simulate RSO motion in various mission scenarios.

The first stationary imaging target is placed in the upper center of the camera field of view resulting in an initial large rotational error about the y-axis. The results of this are shown in Figure 11. The second stationary imaging target was placed to the left of the camera within the field of view and these results of this are shown in Figure 12.

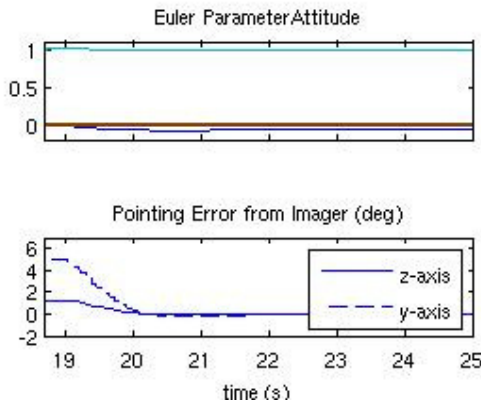


Figure 11 - Stewart Platform Tracking with Large y-axis Rotation

The upper plot for both tracking maneuvers shows the Euler parameter attitude. This attitude was calculated from the measured leg lengths of the platform. The attitude of the satellite has a small overshoot and then converges to the desired attitude. These results are consistent with the inertial attitude change from the reaction wheel simulation.

The lower plot shows the angle error calculated from the pixel error in the images. This error goes to zero as the satellite attitude changes to point at the target.

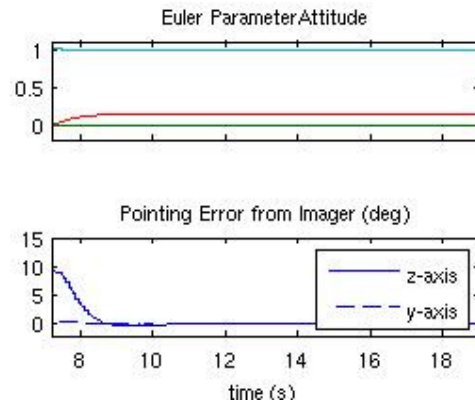


Figure 12 - Stewart Platform Tracking with Large x-axis Rotation

These two hardware-in-the-loop tracking examples demonstrate the feasibility of using the Stewart platform for simulating satellite RSO tracking.

CONCLUSIONS

To demonstrate space-based SSA, the imaging system of the Oculus depends on a stable and precise three-axis control system actuated by reaction wheels. A simulation of the satellite dynamics, sensors, actuators, and control software was developed to test both flight software and hardware components. Simulated inertially-referenced maneuvers of attitude directional changes, rate tracking, and object tracking confirmed calculated control system performance criteria. Visually referenced maneuvers were performance tested with a hardware-in-the-loop, Stewart platform, test bed. These tests not only proved the control system's ability to visually track objects, but more importantly demonstrated a method for testing image-based control systems. Utilizing widely available imagers and associated hardware allows for a simpler and more reliable testing platform by reducing complex hardware simulation. Furthermore this juxtaposition of hardware and software allows system designers to verify and validate flight software outside of a pure simulation environment. Utilizing this hardware-in-the-loop platform for simulating mission scenarios before flying a satellite in space will ultimately help to ensure the success of the Oculus mission.

ACKNOWLEDGEMENTS

The authors would like to thank Dr. Hanspeter Schaub for stimulating and clarifying discussions on the reaction wheel controller.

REFERENCE

1. Shoemaker, J., Space Situational Awareness and Mission Protection. DARPAtech. August 2005, http://www.darpa.mil/DARPAtech2005/presentations/space_act/ (accessed April 2008).
2. The Enterprise Program, <http://www.enterprise.mtu.edu/> (accessed June 2008).
3. "Space Mission Analysis and Design," Edited by J.R. Wertz and W.J. Larson, 364-368, Microcosm and Kluwer, 1999.
4. Baruh, H., Analytical Dynamics, WCB/McGraw-Hill, 1999.
5. Baumgarte, J., "Stabilization of Constraints and Integrals of Motion in Dynamic Systems," Computer Methods in Applied Mechanics and Engineering, 1972: 1-16.
6. Schaub, H., and J.L. Junkins, Analytical Mechanics of Space Systems. Reston, VA: AIAA, 2003.
7. Huang, C.I, C. Chang, M. Yu, and L. Fu, "Sliding-Mode Tracking Control of the Stewart Platform," Control Conference, 2004, 5th Asian, 2004: 562-569 Vol.1.